Perforin-mediated suppression of B-cell lymphoma

Paul Bolitho[a,b], Shayna E. A. Street[a], Jennifer A. Westwood[a], Winfried Edelmann[c], Duncan MacGregor[d,e], Paul Waring[f], William K. Murray[e,g], Dale I. Godfrey[b], Joseph A. Trapani[a,e], Ricky W. Johnstone[a,e], and Mark J. Smyth[a,e,1]

[a]Cancer Immunology Program, Peter MacCallum Cancer Centre, East Melbourne, Victoria 3002, Australia; [b]Department of Microbiology and Immunology, University of Melbourne, Parkville, Melbourne, Victoria 3010, Australia; [c]Department of Cell Biology, Albert Einstein College of Medicine, Bronx, NY 10461; [d]Department of Anatomical Pathology, Austin and Repatriation Medical Centre, Heidelberg, Victoria 3084, Australia; [e]Department of Pathology, University of Melbourne, Parkville, Melbourne, Victoria 3010, Australia; [f]Pathology and Diagnostics, Genentech Incorporated, South San Francisco, CA 94080; and [g]Department of Pathology, Peter MacCallum Cancer Centre, East Melbourne, Victoria 3002, Australia

Edited by James P. Allison, Memorial Sloan-Kettering Cancer Center, New York, NY, and approved December 19, 2008 (received for review September 10, 2008)

In the present study, we have examined the effect of perforin (pfp) deficiency in 4 models of mouse B-cell lymphomagenesis. We have examined pfp loss on the background of either Mlh1 tumor suppressor allele loss or oncogene expression [Ig heavy chain (Eμ)-v-Abl, Eμ-myc, and vav-bcl2]. Pfp was shown to act as a suppressor of B-cell malignancies characteristically driven by v-Abl or bcl-2, whereas Mlh loss cooperated in accelerating spontaneous B-cell lymphomas characteristic of pfp loss. No protective role for pfp was observed in the more aggressive Eμ-myc model of B-cell lymphoma. These transgenic models have allowed us to distinguish the role of pfp in surveillance of B-cell lymphomagenesis, as opposed to its loss simply driving the onset of a spontaneous lymphoma characteristic of pfp deficiency.

tumor surveillance | lymphomagenesis | transgenic mice

Evidence of tumor suppression mechanisms exerted by the immune system has now been reported in several experimental mouse models (1). These experiments have validated and extended the original cancer immune surveillance hypothesis proposed by Burnet (2) and Thomas. More recently, Dunn and Schreiber have proposed a process termed *cancer immunoediting*, which may account for outgrowth of tumors in immunocompetent hosts (3–5). The cancer immunoediting hypothesis predicts a more complex interaction between transformed cells and the host immune system and is thought to consist of 3 distinct phases termed *elimination*, *equilibrium*, and *escape*. Immunoediting of tumors, sculpting them to become less immunogenic, occurs under immune selection pressure, with escaping tumors in WT immunosufficient mice often being less immunogenic than tumors emerging from immunodeficient mice (4). Experimental evidence for the existence of these 3 stages and immunoediting is now mounting (6, 7); however, the exact involvement of each immune cell subset and its effector molecules remains to be fully defined.

Perforin (pfp) is a pore-forming protein of ≈67 kDa that shows some degree of homology to the terminal complement protein C9 (8). Expressed by natural killer (NK) cells, $\gamma\delta^+$T cells, $CD8^+$ cytotoxic T lymphocytes (CTLs), and some other T-cell subsets (9–11), pfp is essential for delivery of proapoptotic granzymes, which initiate the destruction of virus-infected or transformed cells (12–14). We have previously demonstrated that approximately half of a cohort of aging pfp-deficient mice developed spontaneous mature B-cell lymphomas between 300 and 750 days from birth (15–17). This phenotype was reproduced using 2 different gene-targeted mutations and 2 immunologically distinct inbred strains (C57BL/6 or BALB/c), with a small proportion of pfp-deficient mice developing plasmacytomas in the BALB/c strain. Strikingly, an invariant hallmark feature of these lymphomas of B-cell origin was their remarkably unique and high expression of a variety of costimulatory molecules (e.g., CD40, CD70, CD80, CD86) and strong immunogenicity on transplant into WT mice.

It remained unclear from these prior studies whether a loss of pfp was a direct cause of lymphoma or led indirectly to its development as a result of loss of immune surveillance normally mediated by extrinsic cytolytic effector function. The avid ability of WT mice to reject B-cell lymphomas derived from pfp-deficient mice in a pfp-dependent manner when transplanted supported the latter hypothesis. However, all B-cell lymphomas derived from pfp-deficient (15), pfp × β2m-deficient (17), or $p53^{+/-}$ × pfp-deficient (15) mice expressed an uncharacteristically immunogenic phenotype that suggested a peculiar type (or activation state) of B cell was predisposed to malignancy following pfp loss. A loss of p53 alleles(s) accelerated the lymphomagenesis caused by the pfp null mutation rather than a lack of pfp accelerating all tumors caused by p53 allele loss (15). Thus, it remained to be established whether (*i*) pfp was a specific extrinsic suppressor of some or all B-cell malignancies and (*ii*) whether pfp was an effector molecule used by surveilling lymphocytes to regulate the incidence of B-cell lymphoma initiated and characterized by defined tumor suppressor loss or oncogene expression.

We have taken the approach of trying to illustrate that pfp loss could extrinsically regulate prototypic lymphomagenesis driven by defined genetic lesions. Herein, we have examined the impact of pfp deficiency in 4 different C57BL/6 mouse models of B-cell lymphoma. Overall, our data indicate that pfp can act both as an extrinsic suppressor of mature B-cell malignancy characteristically driven by v-abl or bcl-2 expression and cooperatively with intrinsic tumor suppressors like Mlh1 and p53 to suppress B-cell lymphomagenesis characteristic of pfp loss.

Results

Mlh Loss Accelerates B-Cell Lymphomagenesis in Pfp-Deficient Mice. Mlh1 and Msh2 are DNA mismatch repair genes that, when mutated, make individuals highly susceptible to hereditary nonpolyposis colorectal cancer (HNPCC) (18–20). $Mlh1^{-/-}$ mice, similar to HNPCC pedigrees, are also susceptible to gastrointestinal carcinogenesis. However, unlike human $Mlh1^{-/-}$ carriers, $Mlh1^{-/-}$ mouse strains also develop a high proportion of lymphomas and other sporadic tumors (21, 22). We evaluated tumor development in aging C57BL/6 $Mlh1^{+/-}$ $pfp^{+/+}$ and C57BL/6 $Mlh1^{+/-}$ $pfp^{-/-}$ (hereafter referred to as $Mlh^{+/-}$ $pfp^{+/+}$ and $Mlh^{+/-}$ $pfp^{-/-}$, respectively) mice. Similar to a published report (21), 43% of $Mlh^{+/-}$ $pfp^{+/+}$ mice succumbed to

Author contributions: P.B., D.I.G., J.A.T., R.W.J., and M.J.S. designed research; P.B., S.E.A.S., J.A.W., D.M., P.W., W.K.M., and M.J.S. performed research; W.E. contributed new reagents/analytical tools; P.B., S.E.A.S., D.I.G., and M.J.S. analyzed data; and P.B., J.A.T., R.W.J., and M.J.S. wrote the paper.

The authors declare no conflict of interest.

This article is a PNAS Direct Submission.

[1]To whom correspondence should be addressed. E-mail: mark.smyth@petermac.org.

This article contains supporting information online at www.pnas.org/cgi/content/full/0809008106/DCSupplemental.

IMMUNOLOGY

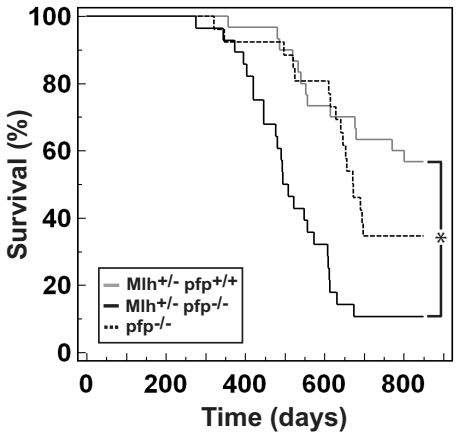

Fig. 1. Mlh heterozygosity accelerates lymphomagenesis in the absence of pfp. Kaplan-Meier curve showing percentage survival of $Mlh^{+/-}$ $pfp^{+/+}$ (n = 30, gray solid line) and $Mlh^{+/-}$ $pfp^{-/-}$ (n = 28, black solid line) mice. Historical control representing lymphoma development in $pfp^{-/-}$ mice (n = 26, black dashed line) is overlaid. Mice were monitored for at least 800 days. Asterisk represents statistically significant difference between $Mlh^{+/-}$ $pfp^{+/+}$ and $Mlh^{+/-}$ $pfp^{-/-}$ groups ($P < 0.0001$, log-rank test).

lymphomas of T- and B-cell origin by 2 years of age [mean age at time of death (MA) = 582 ± 34 days]. Unlike a previous report, when Mlh1 mutant mice backcrossed 2 or 3 generations to C57BL/6 developed a proportion of gastrointestinal tumors (21), no such tumors were observed in either C57BL/6 $Mlh^{+/-}$ $pfp^{+/+}$ or C57BL/6 $Mlh^{+/-}$ $pfp^{-/-}$ mice (backcrossed more than 10 generations to the C57BL/6 genetic background) (Table S1). Notably, a statistically greater proportion (89%; $P < 0.0001$, Fisher's exact test) of $Mlh^{+/-}$ $pfp^{-/-}$ mice died during the same time period (MA = 497 ± 20 days) (Fig. 1). One of our previously aged cohorts of $pfp^{-/-}$ mice was used as a historical control for this and the following 2 aging experiments (MA = 593 ± 28 days; comparable to a similar cohort reported in ref. 15). Histological assessment of fixed tissue from moribund mice revealed that the overwhelming majority of mice on a $pfp^{-/-}$ background had developed lymphoma. Thus, although the time of onset of disease was similar in both strains of mice, the rate of disease progression and the penetrance were greatly increased in mice also lacking pfp ($P < 0.0001$, log-rank test).

$Mlh^{+/-}$ $Pfp^{-/-}$ Mice Develop B-Cell Lymphomas Characteristic of Pfp Loss. Phenotypic assessment of 6 lymphomas arising in $Mlh^{+/-}$ $pfp^{+/+}$ and $Mlh^{+/-}$ $pfp^{-/-}$ mice are shown in Fig. 2*A*. Half of the lymphomas arising in $Mlh^{+/-}$ $pfp^{+/+}$ mice were T cell in origin (1 $CD4^+CD8^+TCR\beta^-$ lymphoma and 2 $CD4^+CD8^-TCR\beta^+$ lymphomas), whereas the remaining 3 lymphomas were of B-cell origin ($CD19^+B220^+$). Notably, all 8 of the $Mlh^{+/-}$ $pfp^{-/-}$ lymphomas assessed were of B-cell origin ($CD19^+B220^+$) and expressed the costimulatory molecules CD86, CD80, CD40, and CD70 (Fig. 2*A*). These B-cell tumors also expressed high levels of MHC class I and MHC class II, very reminiscent of the immunogenic B-cell lymphomas that spontaneously arose in C57BL/6-pfp– and BALB/c-pfp–deficient mice (15, 16).

We next assessed the immunogenicity of each tumor line by secondary transplant into syngeneic C57BL/6 WT or immunocompromised mice (Fig. 2*B*). The T-cell lymphoma MH61 and B-cell lymphoma MH96 derived from $Mlh^{+/-}$ $pfp^{+/+}$ mice grew in all strains transplanted, although the B-cell lymphoma MH81 was avidly rejected in WT mice but grew in RAG-$1^{-/-}$ and $pfp^{-/-}$ mice and in WT mice specifically depleted of CD8 T cells. In contrast to the tumors derived from $Mlh^{+/-}$ $pfp^{+/+}$ mice, all lymphomas that we assessed arising from $Mlh^{+/-}$ $pfp^{-/-}$ mice

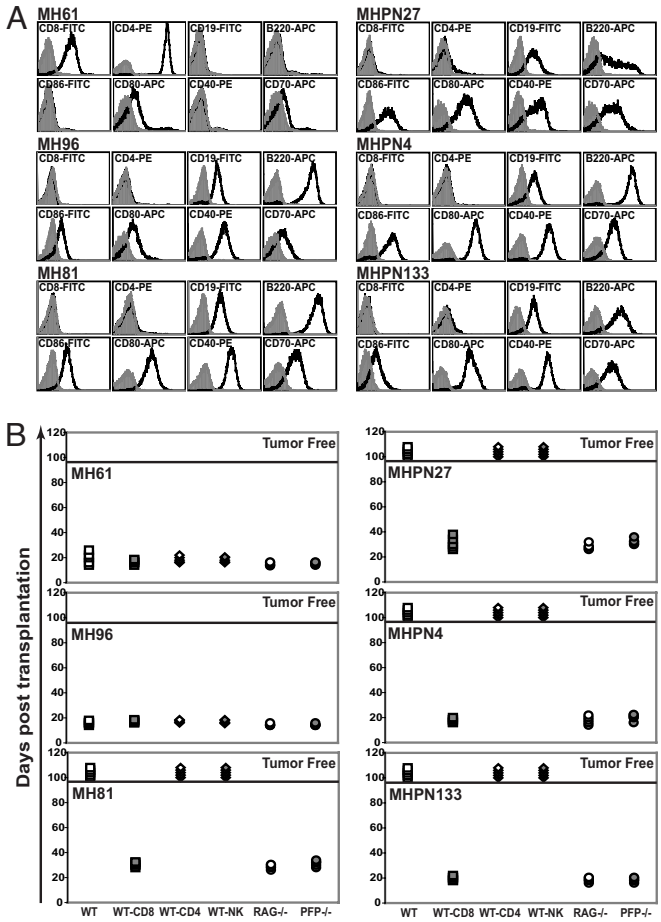

Fig. 2. Lymphomas derived from $Mlh^{+/-}$ $pfp^{-/-}$ mice display an unedited phenotype. (*A*) Flow cytometry data displaying typical cell surface phenotypes of $Mlh^{+/-}$ $pfp^{+/+}$ (MH) and $Mlh^{+/-}$ $pfp^{-/-}$ (MHPN) lymphomas (total n = 3 shown for each tumor type). All samples were derived from enlarged spleens after in vivo passage through C57BL/6 RAG-$1^{-/-}$ mice to obtain a pure tumor population. Shaded histograms represent unstained cells, whereas solid-line histograms represent cells stained with the indicated antibody. (*B*) Immune-mediated rejection analysis of MH and MHPN lymphomas after transplantation (total n = 3 shown for each tumor type). Ten million splenocytes were transferred by i.p. injection into WT mice (open squares), RAG-$1^{-/-}$ mice (open circles), $pfp^{-/-}$ mice (shaded circles), or WT mice with weekly mAb-mediated depletion of CD8 T cells (shaded squares), CD4 T cells (open diamonds), or NK cells (shaded diamonds). Mice were monitored for lymphoma development for 100 days, after which they were declared tumor-free (above solid bar).

were very immunogenic, growing in RAG-$1^{-/-}$ and $pfp^{-/-}$ mice but rejected in WT mice unless they were additionally depleted of CD8 T cells. Taken together, these data suggest that loss of a Mlh1 allele has accelerated the disease process that occurs in the absence of pfp and the lymphomas are characteristic of pfp loss.

Pfp Suppresses v-Abl–Induced Plasmacytoma. Human myelomas overexpress the tyrosine kinase protein, Abl (23), and a proportion of transgenic mice expressing v-Abl, the oncogene product of the Abelson murine leukemia virus under the control of the Ig heavy chain (Eμ) enhancer and the SV40 Tag promoter, develop plasmacytomas with age (24, 25). C57BL/6 mice are normally relatively resistant to plasmacytoma formation, both in transgenic models and in peritoneal irritant-induced tumor models (26–28). We evaluated spontaneous tumor development in aging C57BL/6 Eμ-v-Abl^+ $pfp^{+/+}$ and C57BL/6 Eμ-v-Abl^+ $pfp^{-/-}$ (hereafter referred to as v-Abl^+ $pfp^{+/+}$ and v-Abl^+

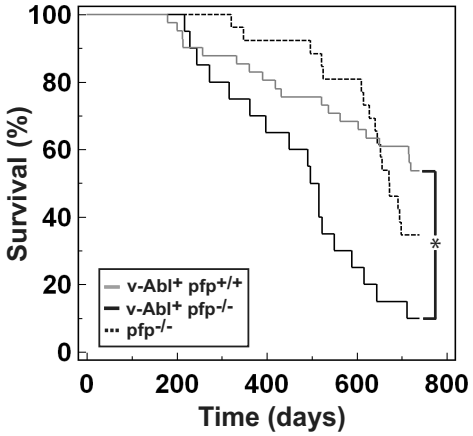

Fig. 3. Loss of pfp accelerates plasmacytoma development in v-Abl$^+$ transgenic mice. Kaplan-Meier curve showing percentage survival of v-Abl$^+$ pfp$^{+/+}$ (n = 41, gray solid line) and v-Abl$^+$ pfp$^{-/-}$ (n = 20, black solid line) mice. Historical control representing lymphoma development in pfp$^{-/-}$ mice (n = 26, black dashed line) is overlaid. Mice were monitored for at least 750 days. Asterisk represents statistically significant difference between v-Abl$^+$ pfp$^{+/+}$ and v-Abl$^+$ pfp$^{-/-}$ groups (P = 0.0003, log-rank test).

pfp$^{-/-}$, respectively) mice that are predisposed to plasmacytoma formation (Fig. 3). In concert with a previous report (28), 17% of v-Abl$^+$ pfp$^{+/+}$ mice (MA = 455 ± 43 days) succumbed to plasmacytomas within 12 months; however, a further 29% of the cohort succumbed between 1 and 2 years of age, with a total of 46% developing plasmacytomas (Fig. 3). By contrast, 30% of v-Abl$^+$ pfp$^{-/-}$ mice (MA = 452 ± 36 days) succumbed to disease by 12 months, and 90% (P = 0.002, Fisher's exact test) were killed with plasmacytomas by 2 years of age (Fig. 3). All tumors from both v-Abl$^+$ pfp$^{+/+}$ and v-Abl$^+$ pfp$^{-/-}$ mice were confirmed histologically as plasmacytomas with characteristic nuclei and prominent eccentric basophilic cytoplasm (Table S2). Thus, pfp sufficiency significantly suppressed plasmacytoma development in Eμ-v-Abl transgenic mice (P = 0.0003, log-rank test).

v-Abl Plasmacytomas Are Edited in a Pfp-Dependent Manner. Similar to a previous report (29), plasmacytomas arising in both v-Abl$^+$ pfp$^{+/+}$ and v-Abl$^+$ pfp$^{-/-}$ mice expressed CD138 (syndecan-1), had little or no cell surface CD19 and B220, displayed reduced levels of surface membrane immunoglobin (mlg), and either failed to express or expressed very low levels of costimulatory molecules. The v-Abl$^+$ pfp$^{+/+}$ plasmacytomas produced IgG and IgA antibodies as previously reported (25), whereas the v-Abl$^+$ pfp$^{-/-}$ lesions that we were able to assess secreted only 1 subclass of IgG (either IgG2a or IgG2b) (Fig. S1).

All 4 v-Abl pfp$^{+/+}$ lines (designated VABL) tested grew in both immunocompetent and immunocompromised mice at the highest dose, suggesting that these tumors were not immunogenic (but subjected to immunoediting) (Fig. 4*A* and Fig. S2). In contrast, 2 of the 3 v-Abl pfp$^{-/-}$ lines (designated PNVABL) tested were avidly rejected on transplantation at the highest dose into WT mice. However, tumor growth proceeded in the absence of pfp or an adaptive immune system (Fig. 4*A*). Tumor rejection of PNVABL1 was dependent on both CD8$^+$ and CD4$^+$ T cells (Fig. 4*B*), in contrast to previous lymphomas that have developed in the absence of pfp, where rejection was only dependent on CD8$^+$ T cells. Consistent with a less immunogenic cell surface phenotype, v-abl pfp$^{-/-}$ lines were less immunogenic when transplanted in WT mice than Mlh$^{+/-}$ pfp$^{-/-}$ lines. Taken together, these data describe a pfp-dependent immunoediting process that occurs during the genesis of Abl-driven plasmacytoma. This is perhaps the best evidence to date that lymphocytes

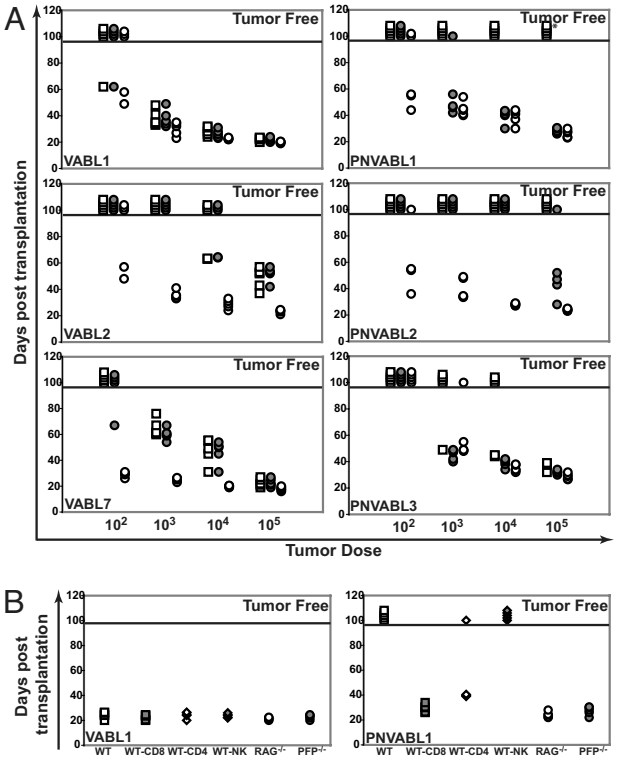

Fig. 4. v-Abl$^+$ pfp$^{-/-}$-derived plasmacytomas display an unedited phenotype. (*A*) Transplantation analysis of v-Abl$^+$ pfp$^{+/+}$ (VABL)- and v-Abl$^+$ pfp$^{-/-}$ (PNVABL)-derived plasmacytomas (total n = 3 shown for each tumor type). All samples were derived from ascites after in vivo passage through C57BL/6 RAG-1$^{-/-}$ mice. Ascites cells were then transferred by i.p. injection into WT mice (open squares), pfp$^{-/-}$ mice (shaded circles), and RAG-1$^{-/-}$ mice (open circles) at the indicated doses. Mice were monitored for plasmacytoma development (abdominal distension) for 100 days, after which they were declared tumor-free (above solid bar). Asterisk represents a PNVABL1 tumor that escaped in 1 WT mouse after 107 days. (*B*) Immune-mediated rejection analysis of VABL and PNVABL plasmacytomas (representative shown for each tumor type). One hundred thousand ascites cells were transferred by i.p. injection into WT mice (open squares), RAG-1$^{-/-}$ mice (open circles), pfp$^{-/-}$ mice (shaded circles), or WT mice with weekly antibody-mediated depletion of CD8 T cells (shaded squares), CD4 T cells (open diamonds), or NK cells (shaded diamonds). Mice were monitored as previously described.

expressing pfp detect and eliminate Abl-transformed plasmacytoma cells, leaving less immunogenic plasmacytoma cells to escape and grow out in the immune competent host.

Pfp Delays Onset of vav-bcl2–Driven Follicular Lymphoma. A hallmark feature of follicular B-cell lymphoma in humans is the t(14, 18) chromosomal translocation, which brings the antiapoptotic proto-oncogene bcl2 under the control of the Eμ locus (30). Interestingly, mice overexpressing bcl2 under the Eμ enhancer are not susceptible to follicular lymphoma but, instead, develop a range of B-lymphoid malignancies, including pre–B-cell lymphomas and plasmacytomas (31). However, follicular lymphoma, with an incidence of up to 50% by 18 months of age, can be simulated in mice by overexpressing bcl2 under the panhematopoietic promoter, vav (32, 33). This represents an animal model for bcl2-induced human follicular lymphoma. Herein, 44% of C57BL/6 vav-bcl2$^+$ pfp$^{+/+}$ (MA = 400 ± 22 days) mice succumbed to lymphoma within 1 year of life (Fig. 5). In contrast, a greater proportion of vav-bcl2$^+$ pfp$^{-/-}$ (MA = 260 ± 14 days) mice had developed lymphoma after 1 year (83%; P = 0.0002, Fisher's exact test). Total disease incidence at the conclusion of the experiment was the same in both strains (100% vs. 97.5% for

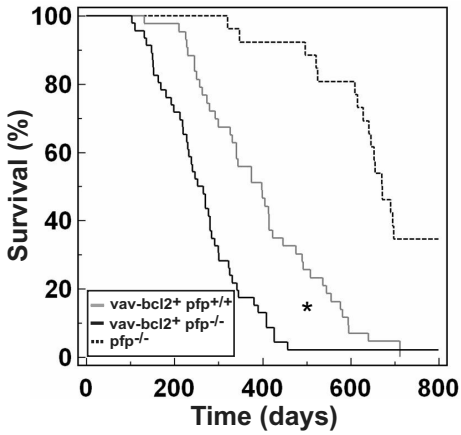

Fig. 5. Loss of pfp accelerates follicular lymphoma development in vav-bcl2$^+$ transgenic mice. Kaplan-Meier curve showing percentage survival of vav-bcl2$^+$ pfp$^{+/+}$ (n = 43, gray solid line) and vav-bcl2$^+$ pfp$^{-/-}$ (n = 46, black solid line) mice. Historical control representing lymphoma development in pfp$^{-/-}$ mice (n = 26, black dashed line) is overlaid. Mice were monitored for at least 800 days. Asterisk represents statistically significant difference between vav-bcl2$^+$ pfp$^{+/+}$ and vav-bcl2$^+$ pfp$^{-/-}$ groups (P = 0.0001, log-rank test).

vav-bcl2$^+$ pfp$^{+/+}$ and vav-bcl2$^+$ pfp$^{-/-}$, respectively; $P > 0.05$, Fisher's exact test). Histological assessment determined follicular lymphoma in each instance (Fig. S3 and Table S3). Thus, pfp influences the speed of onset of vav-bcl2–driven lymphomagenesis (P = 0.0001, log-rank test) but does not prevent overall disease development. Our attempts to grow these lymphomas in immunocompromised mice for further transplant studies were unsuccessful; thus, any differences in immune phenotype or immunogenicity between follicular lymphomas that developed in the presence or absence of pfp could not be determined. Regardless, from the primary tumor data alone, it is likely that the characteristic follicular lymphoma driven by vav-bcl2 was regulated by pfp-mediated immune surveillance.

Pfn Does Not Affect Eμ-myc–Driven Lymphomagenesis. Mice overexpressing c-myc under the control of the IgH enhancer Eμ have an expanded pre–B-lymphocyte pool and develop aggressive pre–B- and B-cell malignancies that closely model Burkitt's lymphoma in humans. The disease is highly penetrant, with 90% of mice developing B-cell tumors within 5 months of age (34). We sought to determine if pfp was able to delay lymphoma development in this transgenic mouse model (Fig. S4 and Table S4). Time to incidence of disease was similar between Eμ-myc$^+$ pfp$^{+/+}$ (MA = 135 ± 27 days), Eμ-myc$^+$ pfp$^{+/-}$ (MA = 118 ± 18 days), and Eμ-myc$^+$ pfp$^{-/-}$ (MA = 139 ± 25 days) mice, and the total penetrance of disease was identical in each strain (94%, 93%, and 90%, respectively). Overall, we observed no influence of pfp on Eμ-myc–driven lymphomagenesis (P = 0.705, log-rank test).

Discussion

Pfp appears to play an important role in NK cell-mediated suppression of tumor metastasis (35), suppression of carcinogen-induced sarcoma (36), and mild suppression of Her2/neu-driven mammary carcinoma (37). However, pfp deficiency leads to an increased rate of spontaneous B-cell malignancy in mice rather than a broader spectrum of tumor types (15, 17). Thus, it was not clear whether pfp loss resulted in a failure in tumor immune surveillance or was causative in lymphomagenesis by simply allowing extended B-cell survival. We have now addressed this issue by using a number of the most relevant mouse models of different B-cell malignancies, where pfp loss cooperates with tumor suppressor loss and/or oncogene activation. The increased plasmacytoma and follicular lymphoma observed in v-abl pfp$^{-/-}$ and vav-bcl2 pfp$^{-/-}$ mice, respectively, illustrated that pfp could regulate lymphomagenesis with a phenotype characteristically driven by oncogene activation.

Our experiments detailing the role of pfp loss in combination with oncogene overexpression appear to reveal a tumor immune surveillance mechanism facilitated by pfp more clearly. Mice overexpressing v-Abl or bcl2, in addition to a lack of pfp, developed lesions either at an accelerated rate with increased penetrance or with an earlier onset when compared with pfp-sufficient transgenic controls. Interestingly, these mice developed plasmacytomas and follicular B-cell tumors characteristic of the oncogene itself rather than those that develop spontaneously with pfp deficiency, suggesting that disease acceleration and/or increased incidence was indeed attributable to failure of an active extrinsic tumor suppression function by pfp. Transgenic mice that lacked pfp never succumbed to immunogenic B-cell lymphomas akin to those that develop spontaneously in the absence of pfp with or without additional tumor suppressor loss. Indeed, these oncogenes are strong drivers of tumorigenesis, and it is possible that the predefined genetic pathway to cancer that exists in these transgenic mice circumvents the perhaps stochastic genetic and molecular programs that are initiated in spontaneous B-cell malignancies typically caused by pfp loss. Transplantation studies of the v-abl–driven plasmacytomas determined that pfp-dependent immunoediting had occurred, further emphasizing the critical importance of pfp as a mediator of immune surveillance in this setting. Thus, these transgenic models allow us to distinguish the role of pfp in surveillance of B-cell lymphomagenesis, as opposed to simply preventing lymphoma onset. The v-abl–driven plasmacytoma is not representative of many human B-cell malignancies; therefore, assessment of the effect of pfp loss in the recently characterized Eμ-XBP-1s and Vk-myc mouse models of multiple myeloma (38–40) is now of great interest.

Allelic heterozygosity at the Mlh1 and p53 loci accelerated disease progression on a pfp-deficient background and, in the case of Mlh1 allelic loss, most obviously increased the overall disease penetrance, with the distinction being that sarcomas account for a large proportion of tumors arising in p53$^{+/-}$ mice and these are not regulated in any significant manner by pfp (15). In both instances, the B-cell lymphomas arising bore a striking immunological resemblance (highly immunogenic on transplantation into WT mice and by cell surface marker characterization) to those that developed spontaneously in mice that were simply pfp-deficient, suggesting that tumor suppressor loss was acting to accelerate the disease that normally proceeds in the absence of pfp. Although this may be strictly true in the case of Mlh1, in which all the tumors from the Mlh$^{+/-}$ pfp$^{-/-}$ mice were highly immunogenic B-cell lymphomas, pfp deficiency did not preclude the development of sarcomas in p53$^{+/-}$ pfp$^{-/-}$ mice (15). At least temporally, it would appear that pfp, Mlh1, and p53 loss could cooperate, because tumors arise concurrently in pfp$^{-/-}$, Mlh$^{+/-}$, and p53$^{+/-}$ mice (from ≈1 year onward); however, loss of a single pfp allele is insufficient to alter the disease pattern on a p53$^{+/-}$ background (15). Thus, it would appear that a minimal level of pfp function serves to effect its control on the mature B-cell compartment and that, in its absence, loss of well-characterized cellular tumor suppressor pathways (e.g., p53, Mlh1) cooperates to drive the malignancy of such B cells. It would be of great interest now to compare loss of p53 or Mlh heterozygosity in tumors that arise in pfp$^{+/+}$, pfp$^{+/-}$, and pfp$^{-/-}$ backgrounds.

No effect was observed for pfp loss in the Eμ-myc model, demonstrating that pfp does not suppress all lymphomas of B-cell origin. The major obvious distinctions are the early onset and high penetrance of Eμ-myc–driven lymphoma and the early

differentiation stage of B cells that emerge as tumors in this model. Thus, pfp clearly suppresses malignancies of mature B-lymphocyte origin, but perhaps pfp has little or no control over the pre–B-cell malignancies that are known to develop in the Eμ-myc model (34). The failure of pfp to prevent Eμ-myc–driven tumors might have been explained by the short disease latency; however, given that loss of NKG2D has been shown to accelerate Eμ-myc lymphoma, this reason seems less likely because NKG2D can clearly suppress lymphoma onset (40). Alternatively, the initiating oncogene myc may trigger pathways that suppress key recognition events or intrinsic apoptotic programs that are necessary for sensitivity to pfp-mediated lymphocyte cytotoxicity. Clearly, the precedent exists, with certain DNA damage pathways leading to stress ligand expression by transformed cells and recognition by effector lymphocytes (41). Deregulated myc expression drives many human cancers, including Burkitt's lymphoma and some highly aggressive diffuse large-cell lymphomas. The Eμ-myc transgenic mouse is a reasonable model for Burkitt's lymphoma, but the human tumor is poorly immunogenic to allogeneic T cells (42). Although intensive chemotherapy is curative for most adult patients with aggressive myc-driven B-cell lymphomas (43), many new therapeutic approaches are being proposed using this mouse model (44). Our findings indicate that underlying immunity to myc-driven B-cell lymphomas should not be overlooked. Further testing of mouse models of early B-cell malignancies and/or those with rapid disease onset may be informative.

Exactly why pfp-deficient mice develop B-cell lymphoma is an important unresolved question, and it is a mystery as to why such emerging B-cell lymphomas are rich in costimulatory molecules, and thus immunogenic on transplantation. A recent report has implicated idiotype-specific T helper 2 cells in the development of B-cell lymphomas, which present their own variable region idiotype peptides in the context of class II MHC (45). Interestingly, these lymphomas closely resembled pfp-deficient lesions in their expression of MHC and costimulatory molecules such as CD80, CD86, and CD40. It will be intriguing to determine whether the spontaneous B-cell lymphomas emerging in mice in the absence of pfp also present idiotypic peptides in their MHC binding grooves. Alternatively, a breakdown in immunoregulation attributable to a lack of pfp-mediated apoptosis may result in uncontrolled hyperplasia within the B-cell compartment, leading to B-cell persistence and eventual malignant transformation in a population of lymphocytes that do have an unusual level of genetic instability as a result of class switching and somatic hypermutation. Notably, $CD4^+$ $CD25^+$ $FoxP3^+$ T-regulatory cells (Tregs) express pfp (11) and are reportedly capable of selectively eliminating activated B lymphocytes in a pfp/granzyme-dependent manner (46). It may now be interesting to compare tumor development in conventional pfp-deficient mice with that in mice conditionally deficient in pfp only in particular lymphocytes subsets such as NK cells, $CD8^+$ T cells, and Tregs (by FoxP3-cre).

In humans, inherited pfp mutations result in a complex severe immune dysregulation that manifests as familial hemophagocytic lymphohistiocytosis (FHL). That syndrome appears to stem from the inability of activated CTLs to eradicate antigen-presenting targets, causing an uncontrolled expansion of T cells and macrophages and, subsequently, a marked elevation of circulating cytokine levels and severe anemia (hemophagocytosis) in the bone marrow and lymphoid organs (47). It has been suggested that FHL might be initiated by a combination of genetic and environmental factors (i.e., certain pathogens controlled by pfp). Although pfp-deficient mice have increased sensitivity to many pathogens compared with WT mice, they only develop a FHL-like syndrome following infection with high doses of certain pathogens such as lymphochoriomeningitis virus (48, 49). This indirect immunoregulatory, rather than classical effector, role of pfp could also lead to tumor formation should it fail. To date, no study in humans has revealed an increased predisposition to B-cell malignancy with pfp polymorphism or mutation. A small but interesting population to assess lymphoma and other tumor development will be those individuals with partial pfp loss who do not succumb to early-onset FHL (47). The prospect of whether pfp influences the development of some human B-cell tumors remains an open question.

Collectively, our study has strengthened the evidence supporting pfp as a potent immunological suppressor of lymphoid malignancies of B-cell origin in the mouse. Using oncogene overexpression, we have distinguished a role for pfp in surveillance of B-cell lymphomas, as opposed to pfp loss being causative of lymphoma.

Methods

Mice and Aging Experiments. C57BL/6 WT mice were either purchased from the Walter and Eliza Hall Institute of Medical Research (WEHI) or bred at the Peter MacCallum Cancer Centre (Peter Mac). C57BL/6 RAG-1–deficient (RAG-$1^{-/-}$) mice and C57BL/6 pfp-deficient ($pfp^{-/-}$) mice [generated from targeted C57BL/6 ES cells as previously reported (14)] were maintained and bred at the Peter Mac. C57BL/6 $Mlh1^{+/-}$ mice (obtained from the Albert Einstein College of Medicine, New York, NY) were backcrossed to C57BL/6 for a total of 10 generations. C57BL/6 $Mlh^{+/-}$ $pfp^{-/-}$ mice were then generated by breeding C57BL/6 $Mlh^{+/-}$ mice with C57BL/6 $pfp^{-/-}$ mice and intercrossing the resulting double-heterozygous offspring to obtain C57BL/6 $Mlh^{+/-}$ $pfp^{+/+}$ and C57BL/6 $Mlh^{+/-}$ $pfp^{-/-}$ mice. C57BL/6 Eμ-v-Abl^+ transgenic mice (backcrossed for at least 12 generations) were obtained from Alan Harris (WEHI, Parkville, Australia). C57BL/6 v-Abl^+ $pfp^{-/-}$ mice were generated by mating C57BL/6 v-Abl^+ mice with C57BL/6 $pfp^{-/-}$ mice and then intercrossing the resulting C57BL/6 v-Abl^+ $pfp^{+/-}$ progeny. The resulting C57BL/6 v-Abl^+ $pfp^{+/+}$ and C57BL/6 v-Abl^+ $pfp^{-/-}$ mice were then independently inbred to generate cohorts aged in the study. C57BL/6 vav-$bcl2^+$ transgenic mice (backcrossed for at least 10 generations) were obtained from Jerry Adams (WEHI, Parkville, Australia). C57BL/6 vav-$bcl2^+$ $pfp^{-/-}$ mice were generated using a similar breeding strategy to the C57BL/6 v-Abl^+ $pfp^{-/-}$ mice described previously. C57BL/6 Eμ-myc^+ transgenic mice (backcrossed for at least 10 generations) were obtained from Jerry Adams and Alan Harris. C57BL/6 Eμ-myc^+ transgenic male mice were mated to C57BL/6 $pfp^{-/-}$ female mice, and the Eμ-myc^+ $pfp^{+/-}$ offspring were used to generate all the mice used in aging cohorts. Only transgenic male mice were used as breeders for reasons previously described (34), and Eμ-myc^+ transgenic mice of all pfp genotypes were kept and entered into the study. There were no differences in the distribution of the genders in these cohorts of mice. $Pfp^{-/-}$ nontransgenic littermates were kept as a control group. For all these studies performed over the past 5 years, C57BL/6 $pfp^{-/-}$ mice were maintained and aged at the Peter Mac under identical conditions as previously described (15). This same data set was used as a historical control in 3 of these experiments to compare B-cell lymphoma development. All mouse experiments were carried out in accordance with ethical guidelines determined by the Peter Mac Animal Experimental Ethics Committee. All mice were aged for up to 800 days in a single clean facility at the Peter Mac, and mice were screened for viral, bacterial, and parasitic infections for the entire experiment. The health and weight of aging mice were monitored twice weekly. Mice were killed at the earliest sign of abnormality (e.g., abdominal distension, enlarged nodes, palpable mass, ruffled fur, labored breathing, greater than 10% weight loss), and the age was recorded. A full autopsy was performed at death, and tumor (macroscopically detected), spleen, liver, thymus, and lymph nodes were routinely examined by histology of formalin-fixed tissues. Single-cell suspensions of lymphoid tissue (typically lymph node or spleen) were often frozen for further flow cytometry phenotyping and transplantation experiments.

Tumor Transplantation Experiments. For C57BL/6 $Mlh^{+/-}$ $pfp^{+/+}$ (MH)- and C57BL/6 $Mlh^{+/-}$ $pfp^{-/-}$ (MHPN)-derived tumors, 1×10^7 splenocytes from RAG-$1^{-/-}$ passaged mice were transplanted by i.p. injection in PBS into groups of 5 WT, $pfp^{-/-}$, or RAG-$1^{-/-}$ mice. Immune cell subsets were depleted in some groups of WT mice by i.p. injection, beginning at days -1 and 0, of 100 μg of either anti-CD4 (GK1.5), anti-CD8 (53–6.7), or anti-NK1.1 (PK136) mAbs and weekly thereafter until day 56. This protocol efficiently depletes CD4, CD8, or NK cells, respectively. Mice were monitored for signs of lymphoma development (e.g., abdominal distension, ruffled fur) for at least 100 days before being considered tumor-free. Three MH lines (designated MH61, MH96, and MH81) and 3 MHPN lines (designated MHPN27, MHPN4, and MHPN133) were

examined in this manner. For C57BL/6 v-Abl^{+} pfp$^{+/+}$ (VABL)- and C57BL/6 v-Abl^{+} pfp$^{-/-}$ (PNVABL)-derived tumor cell lines, ascites cells from tumor-bearing C57BL/6 RAG-1$^{-/-}$ mice were transplanted by i.p. injection in PBS at the indicated doses into groups of 5 WT, pfp$^{-/-}$, or RAG-1$^{-/-}$ mice. Four VABL lines (designated VABL1, VABL2, VABL5, and VABL7) and 3 PNVABL lines (designated PNVABL1, PNVABL2, and PNVABL3) were tested in this manner. Immune cell subsets were depleted in some groups of WT mice (as above) receiving VABL1 and PNVABL1. Mice were monitored for signs of plasmacytoma development (abdominal distension) for at least 100 days before being considered tumor-free.

ACKNOWLEDGMENTS. We acknowledge Dr. Jerry Adams and Dr. Alan Harris for their generous gift of the transgenic mouse strains used in this study. We also thank our colleagues in the Cancer Immunology Program and the staff of the Peter MacCallum Cancer Centre animal facility and the microscopy imaging and research core facility for valuable technical assistance and intellectual advice that has contributed to this work. We acknowledge Robert D. Schreiber of the Washington University School of Medicine for critical review of this manuscript. P.B. is supported by a Cancer Research Institute Predoctoral Emphasis in Tumor Immunology Scholarship. D.I.G., R.W.J., and M.J.S. are supported by Research Fellowships and a Program Grant from the National Health and Medical Research Council of Australia.

1. Swann JB, Smyth MJ (2007) Immune surveillance of tumors. *J Clin Invest* 117:1137–1146.
2. Burnet FM (1970) The concept of immunological surveillance. *Prog Exp Tumor Res* 13:1–27.
3. Shankaran V, *et al.* (2001) IFNgamma and lymphocytes prevent primary tumour development and shape tumour immunogenicity. *Nature* 410:1107–1111.
4. Dunn GP, *et al.* (2002) Cancer immunoediting: From immunosurveillance to tumor escape. *Nat Immunol* 3:991–998.
5. Smyth MJ, Dunn GP, Schreiber RD (2006) Cancer immunosurveillance and immunoediting: The roles of immunity in suppressing tumor development and shaping tumor immunogenicity. *Adv Immunol* 90:1–50.
6. Dunn GP, *et al.* (2005) A critical function for type I interferons in cancer immunoediting. *Nat Immunol* 6:722–729.
7. Koebel CM, *et al.* (2007) Adaptive immunity maintains occult cancer in an equilibrium state. *Nature* 450:903–907.
8. Masson D, Tschopp J (1985) Isolation of a lytic, pore-forming protein (perforin) from cytolytic T-lymphocytes. *J Biol Chem* 260:9069–9072.
9. Podack ER, Konigsberg PJ (1984) Cytolytic T cell granules. Isolation, structural, biochemical, and functional characterization. *J Exp Med* 160:695–710.
10. Nakata M, *et al.* (1990) Constitutive expression of pore-forming protein in peripheral blood gamma/delta T cells: Implication for their cytotoxic role in vivo. *J Exp Med* 172:1877–1880.
11. Grossman WJ, *et al.* (2004) Human T regulatory cells can use the perforin pathway to cause autologous target cell death. *Immunity* 21:589–601.
12. Kawasaki A, Shinkai Y, Yagita H, Okumura K (1992) Expression of perforin in murine natural killer cells and cytotoxic T lymphocytes in vivo. *Eur J Immunol* 22:1215–1219.
13. Jenne D, *et al.* (1988) Identification and sequencing of cDNA clones encoding the granule-associated serine proteases granzymes D, E, and F of cytolytic T lymphocytes. *Proc Natl Acad Sci USA* 85:4814–4818.
14. Kagi D, *et al.* (1994) Cytotoxicity mediated by T cells and natural killer cells is greatly impaired in perforin-deficient mice. *Nature* 369:31–37.
15. Smyth MJ, *et al.* (2000) Perforin-mediated cytotoxicity is critical for surveillance of spontaneous lymphoma. *J Exp Med* 192:755–760.
16. Street SE, Trapani JA, MacGregor D, Smyth MJ (2002) Suppression of lymphoma and epithelial malignancies effected by interferon gamma. *J Exp Med* 196:129–134.
17. Street SE, *et al.* (2004) Innate immune surveillance of spontaneous B cell lymphomas by natural killer cells and gammadelta T cells. *J Exp Med* 199:879–884.
18. Bronner CE, *et al.* (1994) Mutation in the DNA mismatch repair gene homologue hMLH1 is associated with hereditary non-polyposis colon cancer. *Nature* 368:258–261.
19. Fishel R, *et al.* (1993) The human mutator gene homolog MSH2 and its association with hereditary nonpolyposis colon cancer. *Cell* 75:1027–1038.
20. Papadopoulos N, *et al.* (1994) Mutation of a mutL homolog in hereditary colon cancer. *Science* 263:1625–1629.
21. Edelmann W, *et al.* (1999) Tumorigenesis in Mlh1 and Mlh1/Apc1638N mutant mice. *Cancer Res* 59:1301–1307.
22. Prolla TA, *et al.* (1998) Tumour susceptibility and spontaneous mutation in mice deficient in Mlh1, Pms1 and Pms2 DNA mismatch repair. *Nat Genet* 18:276–279.
23. De Vos J, *et al.* (2002) Comparison of gene expression profiling between malignant and normal plasma cells with oligonucleotide arrays. *Oncogene* 21:6848–6857.
24. Harris AW, *et al.* (1990) Lymphoid tumorigenesis by v-abl and BCR-v-abl in transgenic mice. *Curr Top Microbiol Immunol* 166:165–173.
25. Rosenbaum H, *et al.* (1990) An E mu-v-abl transgene elicits plasmacytomas in concert with an activated myc gene. *EMBO J* 9:897–905.
26. Harris AW, *et al.* (1997) Lymphomas and plasmacytomas in transgenic mice involving bcl2, myc and v-abl. *Curr Top Microbiol Immunol* 224:221–230.
27. Potter M, Pumphrey JG, Bailey DW (1975) Genetics of susceptibility to plasmacytoma induction. I. BALB/cAnN (C), C57BL/6N (B6), C57BL/Ka (BK), (C times B6)F1, (C times BK)F1, and C times B recombinant-inbred strains. *J Natl Cancer Inst* 54:1413–1417.
28. Symons RC, *et al.* (2002) Multiple genetic loci modify susceptibility to plasmacytoma-related morbidity in E(mu)-v-abl transgenic mice. *Proc Natl Acad Sci USA* 99:11299–11304.
29. Chen-Kiang S (2003) Cell-cycle control of plasma cell differentiation and tumorigenesis. *Immunol Rev* 194:39–47.
30. Bakhshi A, *et al.* (1985) Cloning the chromosomal breakpoint of t(14;18) human lymphomas: Clustering around JH on chromosome 14 and near a transcriptional unit on 18. *Cell* 41:899–906.
31. Strasser A, Harris AW, Cory S (1993) E mu-bcl-2 transgene facilitates spontaneous transformation of early pre-B and immunoglobulin-secreting cells but not T cells. *Oncogene* 8:1–9.
32. Ogilvy S, *et al.* (1999) Constitutive Bcl-2 expression throughout the hematopoietic compartment affects multiple lineages and enhances progenitor cell survival. *Proc Natl Acad Sci USA* 96:14943–14948.
33. Egle A, *et al.* (2004) VavP-Bcl2 transgenic mice develop follicular lymphoma preceded by germinal center hyperplasia. *Blood* 103:2276–2283.
34. Harris AW, *et al.* (1988) The E mu-myc transgenic mouse. A model for high-incidence spontaneous lymphoma and leukemia of early B cells. *J Exp Med* 167:353–371.
35. Smyth MJ, *et al.* (1999) Perforin is a major contributor to NK cell control of tumor metastasis. *J Immunol* 162:6658–6662.
36. Street SE, Cretney E, Smyth MJ (2001) Perforin and interferon-gamma activities independently control tumor initiation, growth, and metastasis. *Blood* 97:192–197.
37. Street SE, *et al.* (2007) Host perforin reduces tumor number but does not increase survival in oncogene-driven mammary adenocarcinoma. *Cancer Res* 67:5454–5460.
38. Carrasco DR, *et al.* (2007) The differentiation and stress response factor XBP-1 drives multiple myeloma pathogenesis. *Cancer Cell* 11:349–360.
39. Chesi M, *et al.* (2008) AID-dependent activation of a MYC transgene induces multiple myeloma in a conditional mouse model of post-germinal center malignancies. *Cancer Cell* 13:167–180.
40. Guerra N, *et al.* (2008) NKG2D-deficient mice are defective in tumor surveillance in models of spontaneous malignancy. *Immunity* 28:571–580.
41. Gasser S, Orsulic S, Brown EJ, Raulet DH (2005) The DNA damage pathway regulates innate immune system ligands of the NKG2D receptor. *Nature* 436:1186–1190.
42. Grigg A, Ritchie D (2004) Graft-versus-lymphoma effects: Clinical review, policy proposals, and immunobiology. *Biol Blood Marrow Transplant* 10:579–590.
43. Bishop PC, Rao VK, Wilson WH (2000) Burkitt's lymphoma: Molecular pathogenesis and treatment. *Cancer Invest* 18:574–583.
44. Mason KD, *et al.* (2008) In vivo efficacy of the Bcl-2 antagonist ABT-737 against aggressive Myc-driven lymphomas. *Proc Natl Acad Sci USA* 105:17961–17966.
45. Zangani MM, *et al.* (2007) Lymphomas can develop from B cells chronically helped by idiotype-specific T cells. *J Exp Med* 204:1181–1191.
46. Zhao DM, Thornton AM, DiPaolo RJ, Shevach EM (2006) Activated CD4+CD25+ T cells selectively kill B lymphocytes. *Blood* 107:3925–3932.
47. Voskoboinik I, Smyth MJ, Trapani JA (2006) Perforin-mediated target-cell death and immune homeostasis. *Nat Rev Immunol* 6:940–952.
48. Badovinac VP, Hamilton SE, Harty JT (2003) Viral infection results in massive CD8+ T cell expansion and mortality in vaccinated perforin-deficient mice. *Immunity* 18:463–474.
49. Jordan MB, Hildeman D, Kappler J, Marrack P (2004) An animal model of hemophagocytic lymphohistiocytosis (HLH): CD8+ T cells and interferon gamma are essential for the disorder. *Blood* 104:735–743.